

## Examination of warm transfer on extending sheet by variation iteration method strategy and investigation of arrangements for optimizing liquid properties

Pooya Pasha , Ali Hosin Alibak , Hossein Nabi, Farzad Tat ShahdostFirst published: 23 February 2022 | <https://doi.org/10.1002/eng2.12505>[Early View](#)

Online Version of Record before inclusion in an issue

e12505



Figures



References



Related



Information

### Abstract

This study aimed at investigating the variation of heat transfer and velocity changes of the fluid flow along the vertical line on a surface drawn from both sides. In the beginning, several parameters such as Prandtl number and viscoelastic effect were evaluated for heat transfer and fluid velocity by the variation iteration method. The results were compared with the numerical method. The second part of the description relates to the use Response surface method (RSM method) in the Design Expert software. In this paper, by using the RSM, optimized the fluid velocity and heat transfer passing from the stretching sheet. By increasing the Prandtl number, the convection heat transfer by 43% increased the ratio of the minimum Prandtl number. By balanced modes for Prandtl number and viscoelastic parameter and wall temperature, the best optimization occurred for fluid velocity and fluid temperature with  $f = 0.67$  and  $\theta = 0.606$ . The results of the Variation Iteration method are accurate for the nonlinear solution. As the value of  $k$  increases, the value of fluid velocity increased and by increasing the Prandtl number, the value of temperature decreases.

### 1 INTRODUCTION

Concerning the advancement of science and innovation, we are always seeking out a strategy to arrange to supply mechanical items with low time and great quality. Taking after this, science has remarked able advance in different areas. One of the sciences in which good progress is made is liquid mechanics. The impacts of the liquid stream field on the stretching sheet pulled in numerous analyst considerations so that extensive research was carried out. The compilations of fluid mechanics science and industrial issues have solved engineering important problems. Most linear and nonlinear fluid problems have been solved by the Akbari–Ganji's method, Homotopy perturbation method strategy, and Adomian Decomposition method, like in Maple software. These answers are of great help in industries. Studying warm exchange and liquid stream on an extending sheet applied to hot rolling, refinery, shaping, and the like has helped global scholars and students in using these finding solutions for engineering and industrial concerns for the convergence of their solution be much better. Magneto hydrodynamic (MHD) is one of the contexts that are related to fluid magnetic science. It is a new major that is used in the aerospace industry. In addition, MHD is one of the methods that can influence heat and flow on a stretching sheet.<sup>1–5</sup> Naikoti Kishan et al.<sup>6</sup> investigated MHD impact the warm exchange over a extending sheet rooted in a permeable medium with variable viscosity. Similarly, Stanford Shateyi et al.<sup>7</sup> focused on the numerical investigation of three-dimensional MHD nanofluid stream over a extending sheet with convective boundary circumstances by means of a permeable medium.. Moreover, Makinde et al.<sup>8</sup> evaluated the numerical investigations of unsteady hydro magnetic radiating liquid stream passing an elusive extending sheet rooted in a permeable medium. The display work considers the impacts of the warm radiation, velocity slip, buoyancy force, and heat source. Jalilpour et al.<sup>9</sup> investigated Warm generation/absorption on MHD stagnation stream of nanofluid toward a permeable extending sheet. They researched into MHD stagnation-point stream of a nanofluid via a heated permeable extended sheet with suction or blowing circumstances. Likewise, Nadeem et al.<sup>10</sup> assessed the flow of a Williamson fluid over a extending sheet. Additionally, Cortell<sup>11</sup> investigated the warm and stream exchange of a viscoelastic fluid over a stretching sheet and indicated the transformation of the administering halfway differential equations into conventional differential equations via similitude changes. Tousiflqra et al.<sup>12</sup> also investigated the magnet of the hydrodynamic free stream of nanofluid stream over the exponentially radiating extending sheets with variable liquid features. M. Veera Krishna et al.<sup>13</sup> researched Hall and ion slip impacts on unsteady MHD free convective rotating stream through a saturated porous medium. The present study has an immediate application in understanding the drag experienced at the heated and inclined surfaces in a seepage flow. Masood Khan and Azzam Shahzad<sup>14</sup> examined the boundary later stream of a Sisko liquid over a stretching surface. Iqbal et al.<sup>15</sup> evaluated stagnation-point flow through exponentially stretching sheets by existing thermal radiation and viscous dissipation. In addition, Fayyadh et al.<sup>16</sup> considered performance of the  $Al_2O_3$  crude oil on the nonlinear stretching sheet. Dutta and Gutta<sup>17</sup> also investigated the cooling of a extending surface in a viscous stream. After studying the Stagnation point stream of a micropolar liquid toward a stretching surface, Rosalinda et al.<sup>18</sup> reported that the resulting equations of nonlinear conventional coupled differential equations are numerically solved utilizing the Keller-box method. Ganji and Hatami<sup>19</sup> conducted the squeezing Cu-water nanofluid stream analysis within parallel plots with the differential transform-technique. Khan and Pop<sup>20</sup> addressed the nanofluids boundary-layer stream within a stretching surface. The model utilized for the nanofluid joins the impacts of thermophoresis and Brownian motion. Tanzila et al.<sup>21</sup> also confirmed the induced magnetic field stagnation point stream of nanofluid passing a convectively warmed stretching surface with boundary impacts. Bujurke and Biradar<sup>22</sup> investigated second-order stream flow passing a stretching surface with heat transfer. The warm exchange within a second-order stream flow based on Noll and Coleman constitutive equation was investigated in terms of the postulate of progressively fading memory over a stretching surface. Moreover, Manzoor Ahmed et al.<sup>23</sup> performed steady heat and flow transfer owing to a bidirectional stretching sheet. This project describes the flow of fluid passing through a solid surface. At the solid sheet, as the value of  $y$  increases, the temperature and velocity also change, which is solved by variation iteration method (VIM) method. Pooya Pasha et al.<sup>24</sup> examined the analytical solution of non-Newtonian second-grade fluid flow with variation iteration strategy and Adomian decomposition strategy methods on a stretching surface. This consideration pointed at exploring the variety of warm exchange and speed changes of the liquid stream speed along the vertical line on a plane drawn from both sides. Seyyed Habibollah Hashemi and Domairry Ganji<sup>25</sup> studied the nonlinear equations in streams, advance in nonlinear science. In this book, they investigated a lot of nonlinear equations by maple software. Ghadikolaei et al.<sup>26</sup> evaluated the non-Newtonian second-grade stream flow's numerical and expository solution over a stretching sheet. They compared the results of solving the velocity and temperature equations in the presence of  $k$  changes through Homotopy perturbation method and Numerical method. Chamoli<sup>27</sup> inspected the inclination determination list approach for optimization of  $V$  down punctured, perplexed. The main question in this paper is that what is the relationship between the viscoelastic parameter and Prandtl number with fluid temperature and fluid velocity or in what values of the Prandtl number and viscoelastic

parameter do we reach the optimal state for heat convection from the surface? This study aimed at investigating the variation of heat transfer and velocity changes of the fluid flow along the vertical line on a surface drawn from both sides, also by using the specific data from the viscoelastic parameter, we optimized the speed and warm transfer on the screen wall in different parts of it and check the heat flux from different points by the VIM. The results of the VIM are accurate for the nonlinear solution. The second part of the description relates to the use of the Response Surface method (RSM) in the Design Expert software. In this paper, by using the RSM, optimized the fluid velocity and heat transfer passing from the stretching sheet. The novelty of this paper is the examination of the numerical and analytical differential equations (momentum equation and energy equation) by the VIM methods and finite element method and compares these results with the NUM method. Also, by balanced modes for Prandtl number and viscoelastic parameter and wall temperature, the best optimization occurred for fluid velocity and fluid temperature with  $f = 0.67$  and  $\theta = 0.606$ .

## 2 MATHEMATICAL FORMULATION

### 2.1 Fluid flow analysis

Using the following two equations including fluid and thermal terms, the fluid passing through the surface and the heat from  $y = 0$  to  $y > 0$  is examined in this example:

$$\frac{\partial u^*}{\partial x} + \frac{\partial v^*}{\partial y} = 0, \quad (1)$$

$$u^* \frac{\partial u^*}{\partial x} + v^* \frac{\partial v^*}{\partial y} = \theta \frac{\partial^2 u^*}{\partial y^2} + \frac{\alpha_1}{\rho} \left[ \frac{\partial}{\partial x} \left( u^* \frac{\partial^2 u^*}{\partial y^2} \right) + \frac{\partial u^*}{\partial y} \frac{\partial^2 v^*}{\partial y^2} + \theta \frac{\partial^3 u^*}{\partial y^3} \right], \quad (2)$$

where  $u^*$ ,  $v^*$ ,  $\theta$ , and  $\rho$  represent the velocity factor in the  $x$  course, the velocity factor in the  $y$  direction, kinematic viscosity, and density, respectively:

$$U^* = CX, v^* = 0, \text{ at } y = 0, C > 0. \quad (3)$$

$$U^* \rightarrow 0, \frac{\partial u^*}{\partial y} \rightarrow 0 \text{ at } y \rightarrow \infty. \quad (4)$$

Condition (4) increases when the amplitude of the fluid flow is infinite:

$$U^* = cx f'(\eta), v^* = -(c\theta)^{\frac{1}{2}} f(\eta), \quad (5)$$

where:

$$\eta = \left( \frac{c}{\theta} \right)^{\frac{1}{2}} y. \quad (6)$$

And replacing in Equation (2)<sup>26</sup>:

$$(f')^2 - ff'' = f''' + k[2f'f'' - (f'')^2 - ff'''']. \quad (7)$$

$$f = 0, f' = 1 \text{ at } \eta = 0. \quad (8)$$

$$f' \rightarrow 0, f'' \rightarrow 0 \text{ at } \eta \rightarrow \infty. \quad (9)$$

### 2.2 Heat transfer flow analysis

Energy equation with temperature changes with viscous dissipation:

$$U^* \frac{\partial T^*}{\partial x} + v^* \frac{\partial T^*}{\partial y} = \alpha \frac{\partial^2 T^*}{\partial y^2} + \frac{\theta}{c_p} \left( \frac{\partial u^*}{\partial y} \right)^2, \quad (10)$$

where  $\alpha$  and  $c_p$  are the thermal diffusivity and the special heat of the fluid, respectively. The boundary conditions are:

$$T^* = T_w^*(T_\infty^* + Ax^s) \text{ at } y = 0, T^* \rightarrow T_\infty^* \text{ as } y \rightarrow \infty. \quad (11)$$

The parameter  $s$  denotes the wall temperature.

Prandtl number and  $\theta$ ,

$$\theta(\eta) = \frac{T_w^* - T_\infty^*}{T_w^* - T_\infty^*}, \sigma = \frac{\beta}{\alpha}. \quad (12)$$

Equations (5), (6), (12), and (11) can be written<sup>26</sup>:

$$\theta'' + \sigma f \theta' - s \sigma f' \theta = -\sigma E_c (f'')^2 x^{2-s}. \quad (13)$$

$$\theta(0) = 1, \theta(\infty) \rightarrow 0. \quad (14)$$

With  $E_c = c^2 / A c_p$ :

If  $s = 2$ , we have<sup>14</sup>:

$$\theta'' + \sigma f \theta' - 2 \sigma f' \theta = -\sigma E_c (f'')^2. \quad (15)$$

According to the above formulas, the right-hand part of Equation (1) equals zero, thus the equation is rewritten as follows:

$$\theta'' + \sigma f \theta' - 2 \sigma f' \theta = 0. \quad (16)$$

For negligible dissipation, we have since (13)<sup>14</sup>:

$$\theta'' + \sigma f \theta' - s \sigma f' \theta = 0. \quad (17)$$

### 3 MATHEMATICAL PROCEDURE

#### 3.1 Runge–Kutta method

Runge–Kutta methods are a family of iterative methods used to match solutions to ordinary differential equations. These methods use discretization in computing solutions in small steps. The next step approximation is derived from the previous step by adding  $s$  terms. A problem of initial value should be specified as follows:

$$k_1 = h f(x_n, y_n). \quad (18)$$

$$k_2 = h f\left(x_n + \frac{1}{2}h, y_n + \frac{1}{2}k_1\right). \quad (19)$$

$$k_3 = h f\left(x_n + \frac{1}{2}h, y_n + \frac{1}{2}k_2\right). \quad (20)$$

$$k_4 = h f(x_n + h, y_n + k_3). \quad (21)$$

$$y_{n+1} = y_n + \frac{1}{6}k_1 + \frac{1}{3}k_2 + \frac{1}{3}k_3 + \frac{1}{6}k_4 + O(h^5). \quad (22)$$

$K_1$  is the slope at the start of the space using  $y$ .  $K_2$  is the gradient in the middle of the range using  $y$  and  $k_1$ .  $K_3$  is again the mid-course gradient but using  $y$  and  $k_2$ .  $K_4$  is the slope at the end of the range utilizing  $y$  and  $k_3$ .

#### 3.2 Variation iteration method

Where  $\Omega$  is the frequency angle oscillator. The general formula for obtaining other sentences of  $u$  is defined by a coefficient  $\lambda$  as follows<sup>25</sup>:

$$u' + \Omega^2 u = F(u) \quad F(u) = \Omega^2 u - f(u). \quad (23)$$

Given the boundary equations<sup>25</sup>:

$$u' = 0, \quad u(0) = A. \quad (24)$$

And the first functions<sup>25</sup>:

$$u_0(t) = A \cos \Omega t. \quad (25)$$

$$\int_0^T \cos \Omega t [\Omega^2 u_0 - f(u_0)] dt = 0. \quad (26)$$

The  $\lambda$  coefficient is obtained by dividing the Laplace from the linear part of the equation. By different  $n$  definitions, the number of sentences is considered to obtain a better answer:

$$u_{n+1}(t) = u_n(t) + \int_0^t \lambda \left\{ \frac{d^2 u_n}{d\eta^2} + \Omega^2 u_n(\eta) - F_n \right\} d\eta. \quad (27)$$

where  $\lambda$  is the Lagrange coefficient and  $F_n$  is considered various restricted:

$$\frac{d^2 \lambda}{d\eta^2} + \Omega^2 \lambda(\eta) = 0$$

$$\lambda(t) = 0, 1 - \frac{d\lambda}{dt} = 0 \quad (28)$$

The coefficient  $\lambda$  is calculated from the following formula:

$$\lambda = \frac{1}{\Omega} \sin \Omega (\tau - t) \quad (29)$$

Now we are rewriting the formula:

$$u_{n+1}(t) = u_n(t) + \int_0^t \frac{1}{\Omega} \sin \Omega (\tau - t) \left\{ \frac{d^2 u_n}{d\eta^2} + F_n \right\} d\tau. \quad (30)$$

### 3.3 Application of VIM in the problem

To begin with, we set the linear part of the equation to zero:

$$\frac{d^3}{d\eta^3} f_0(\eta) - \left( \frac{d}{d\eta} f_0(\eta) \right) = 0 \quad (31)$$

$$\frac{d^2}{d\eta^2} \theta_0(\eta) - \theta_0(\eta) = 0 \quad (32)$$

And the equations are illuminated by composing boundary conditions for them:

$$\theta_0(0) = 1, \theta_0(\infty) = 0 \quad (33)$$

$$f_0(0) = 0, D(f_0)(0) = 1, D(f_0)(\infty) = 0 \quad (34)$$

The solution is as follows:

$$f_0(\eta) = \frac{-1 + e^\eta}{e^\eta}, \theta_0(\eta) = e^{-\eta} \quad (35)$$

By calculating coefficient  $\lambda$  and gluing into the equation, we have:

$$\lambda_1 = \tau - \eta + 1. \quad (36)$$

$$\lambda_2 = \tau - \eta. \quad (37)$$

For  $k = 0.01, \sigma = 1, s = 2$  :

$$f_1(\eta) = \frac{-1+e^\eta}{e^\eta} - \frac{1}{2} \left( \left(1 - \frac{-1+e^\eta}{e^\eta}\right)^2 - \frac{(-1+e^\eta)\left(-1+\frac{-1+e^\eta}{e^\eta}\right)}{e^\eta} - 1 + \frac{-1+e^\eta}{e^\eta} - 2k\left(1 - \frac{-1+e^\eta}{e^\eta}\right)\left(-1 + \frac{-1+e^\eta}{e^\eta}\right) + k\left(-1 + \frac{-1+e^\eta}{e^\eta}\right)^2 + \frac{k(-1+e^\eta)\left(-1+\frac{-1+e^\eta}{e^\eta}\right)}{e^\eta} \right) \eta^2 \quad (38)$$

$$\theta_1(\eta) = e^{-\eta} + \frac{1}{2} \left( e^{-\eta} - \frac{\sigma(-1+e^\eta)e^{-\eta}}{e^\eta} - s\sigma\left(1 - \frac{-1+e^\eta}{e^\eta}\right)e^{-\eta} \right) \eta^2 + (-\eta + 1) \left( e^{-\eta} - \frac{\sigma(-1+e^\eta)e^{-\eta}}{e^\eta} - s\sigma\left(1 - \frac{-1+e^\eta}{e^\eta}\right)e^{-\eta} \right) \eta \quad (39)$$

$$f(\eta) = -5 \cdot 10^{-7} (\eta + 287.5548) \eta^2 (\eta - 0.40107) (\eta - 3.598882) (\eta - 290.554848) e^{-4\eta} e^{2\eta} - (0.25e - 4 (\eta - 5.84705499443762)) (\eta - 207.937841477261) (\eta^2 + 5.78489647169834\eta + 32.8994987593262) e^{-4\eta} e^{3\eta} + 1e^{4\eta} - 0.00003\eta^6 - 0.00008\eta^5 + 0.0066\eta^4 - 0.0300\eta^3 + 0.0144\eta^2 e^\eta + 0.0035\eta^5 + 0.00008\eta^3 - 0.0007\eta^4 - 0.000008\eta^2 - 0.000096\eta^6 e^{-4\eta} \quad (40)$$

$$\theta(\eta) = 0.5000000000(\eta^2 + 2e^\eta - 2\eta)e^{-2\eta}$$

## 4 RESPONSE SURFACE METHODOLOGY

Reaction Surface Strategy is a bunch of numerical and statistical strategies to adapt experimental data to polynomial models. RSM is considered one of the test modeling strategies. RSM is one of two considered approaches within the plan of tests. In RSM a proper experimental design is used to find a way to assess the interaction and second-degree effects and even the local shape of the studied response sheet. In the meantime, specific goals are seriously pursued, the most important of which is to make strides in the method by finding ideal inputs, solving problems and weaknesses of the process, and stabilizing it. Here, stabilization is a critical concept in quality that implies minimizing the effects of secondary or uncontrollable variables.

## 5 VALIDATION FOR METHODS

According to the above tables (Tables 1-4), our work compares with Ghadikolaei et al.'s work. The amount of computational error in our work is very low compared to Ghadikolaei et al.<sup>26</sup>

**TABLE 1.** The computational error rate of two variation iteration method (VIM) and homotopy perturbation method (HPM) methods (Ghadikolaei et al.<sup>26</sup>) for  $f(\eta)$  in  $k = 0.01, \sigma = 1$

$\eta$	$f_{VIM}$	$f_{HPM}$	Error
0	0	0	0
0.1	0.095609	0.095199	0.00041
0.2	0.018224	0.0181400	0.000084
0.5	0.392692	0.394050	0.001358
1	0.624650	0.633463	0.008813
2	0.862048	0.866679	0.004631
3	0.955493	0.952228	0.003265
4	0.987897	0.983566	0.004331

**TABLE 2.** The computational error rate of two variation iteration method (VIM) and homotopy perturbation method (HPM) (Ghadikolaei et al.<sup>26</sup>) methods for  $f(\eta)$  in  $k = 0.05, \sigma = 1$

$\eta$	$f_{vim}$	$f_{HPM}$	Error
0	0	0	0
0.1	0.0974139	0.095347	0.002066
0.2	0.186463	0.181926	0.004537
0.5	0.391245	0.396374	0.005129
1	0.5944900	0.638833	0.044343
2	0.8487834	0.874736	0.025953
3	0.9770290	0.960288	0.016741
4	1.013844058	0.991097	0.022747

**TABLE 3.** The computational error rate of two variation iteration method (VIM) and homotopy perturbation method (HPM) (Ghadikolaei et al.<sup>26</sup>) methods for  $f(\eta)$  in  $k = 0.09, \sigma = 1$

$\eta$	$f_{VIM}$	$f_{HPM}$	Error
0	0	0	0
0.1	0.097413	0.095495	0.001918
0.2	0.186463	0.182452	0.004011
0.5	0.391245	0.398699	0.007454
1	0.594490	0.644204	0.049714
2	0.848783	0.882793	0.034013
3	0.977029	0.968348	0.008681
4	1.013849	0.998627	0.015213

TABLE 4. The computational error rate of two variation iteration method and homotopy perturbation method (Ghadikolaei et al.<sup>26</sup>) methods for  $f'(\eta)$  in  $k = 0.01$ ,  $\sigma = 1$

$\eta$	$f'_{VIM}$	$f'_{HPM}$	Error
0	1	1	0
0.1	0.917413	0.905495	0.001918
0.2	0.826463	0.812452	0.004011
0.5	0.591245	0.608699	0.007454
1	0.354490	0.364204	0.049714
2	0.148783	0.132793	0.034013
3	0.127029	0.108348	0.008681
4	1.013849	0.118627	0.015213

## 6 RESULTS AND DISCUSSION

This study sought to evaluate the amount of warm exchange and liquid stream velocity through a flat plate with the analytical method, and then compare the results of this method with numerical method. Tables 1–3 present the error rates for the velocity fluid values of the fluid flow in  $k = 0.01$ ,  $k = 0.05$ ,  $k = 0.09$  by comparing the VIM and project. Figure 1 shows the geometry of the issue.

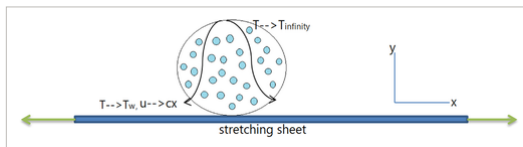
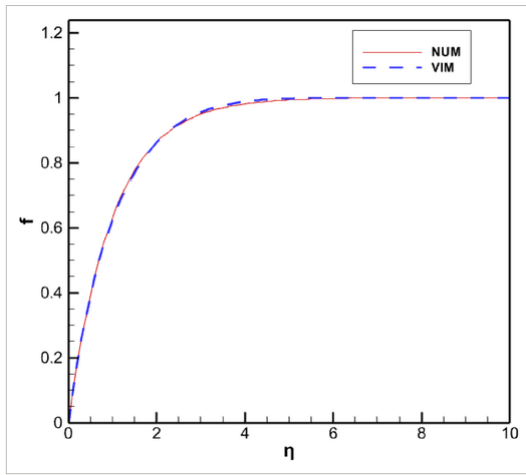


FIGURE 1

[Open in figure viewer](#) | [PowerPoint](#)

Geometry of the problem

First, Figures 2 and 3 compare the results of the VIM and numeric method, and the process of the convergence of pilgrims is plotted. As the value  $\eta$  increases, the lines of these methods approach convergence and are  $\theta(\eta)$  inversely. For example, the comparison between different values of  $k$  in the interval (Figure 4) shows that the rate of velocity increases to one as values tend to zero. At the top of the sheet with decreasing the viscoelastic parameter, the amount of fluid velocity increased, and by passing fluid flow over the stretching surface and by increasing boundary layer at the end of the surface, the value of fluid velocity increased by increasing viscoelastic parameter. Figure 5 shows the effects of changes in the wall temperature parameter for temperature. In this graph, the temperature increases given the decrease in  $s$  (wall temperature). By increasing the distance from the beginning of the surface, the heat transfer and temperature decreased, and it becomes zero at the bottom of the page. Figure 6 displays the effects of changes in the Prandtl number for Temperature for  $k = 0.01$  with an increase in Prandtl in the stretching sheet, the temperature of the liquid decreases. At the top of the sheet and at a distance of  $\eta = 0$  to  $\eta = 2$  by decreasing Prandtl number, the amount of temperature increased, and with spacing from the beginning of the surface ( $\eta = 4$  to  $\eta = 10$ ), the amount of warm transfer increased. Figures 7 and 8 show the effects of changes in the Prandtl number concerning Temperature for  $k = 0.05$  and  $k = 0.09$ . With an increase in Prandtl in the stretching surface, the temperature of the liquid diminishes. The second part of the description relates to the use of RSM in the Design-Expert software. In this paper, by using the RSM optimized the fluid velocity and warm transfer passing from the stretching sheet. To achieve the optimal results of the algorithm, 10 experiments were done in the Design-Expert software by the RSM. With the help of two-dimensional diagrams obtained from fluid parameters like Prandtl number and viscoelastic and wall temperature, the optimal points of velocity and equivalent fluid temperature can be obtained. Figures 9 and 10 show comparisons between actual and experimented results for parameters such as fluid velocity and fluid temperature. Due to the linearity of the curve and the close distances of the data to each other, this experiment is valid, and a very low error is observed between the numbers of actual and experimented results. The purpose of optimization research in this article is to increase heat transfer and reduce fluid flow velocity in specific numbers. In this paper, the response surface method determines the heat transfer and velocity of the passing fluid by generating the input data trend of Prandtl number 0.7–0.9 and viscoelastic parameter 1.25–1.85, and wall temperature of 0.01–0.09. According to Figures 11 and 12, by increasing the viscoelastic parameter from 0.03 to 0.07, the amount of stream velocity increased from  $u = 0.4$  to  $u = 0.7$  at the end of the sheet. Here, the fluid velocity is directly related to the viscoelastic parameter. Based on Figure 13, the amount of warm transfer between the fluid and stretching sheet increases with the distance from the edge of the sheet. Also, as the heat flow passes from the beginning of the plate to the end of the plate, the thickness of the thermal boundary layer increases. Here, the fluid temperature is directly related to the viscoelastic parameter.



**FIGURE 2**

[Open in figure viewer](#) | [PowerPoint](#)

The comparison of answers with variation iteration method and numeric for  $f(\eta)$ ,  $\sigma = 1$ ,  $s = 2$ ,  $k = 0.01$

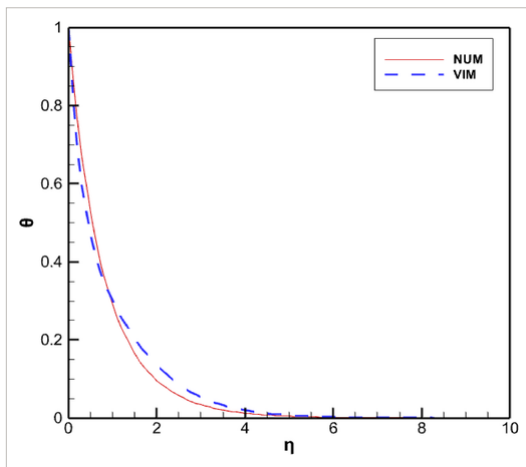


**FIGURE 3**

[Open in figure viewer](#) | [PowerPoint](#)

The comparison of answers by variation iteration method and numeric for  $\Theta(\eta)$ ,  $\sigma = 1$ ,  $s = 2$ ,  $k = 0.01$

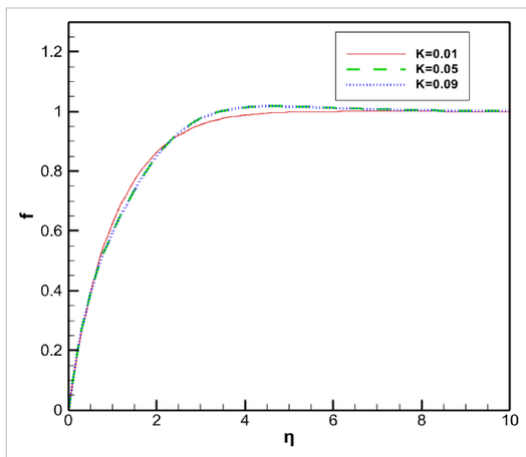


**FIGURE 4**

[Open in figure viewer](#) | [PowerPoint](#)

Velocity profile for several values of  $k$  with  $\sigma = 1$

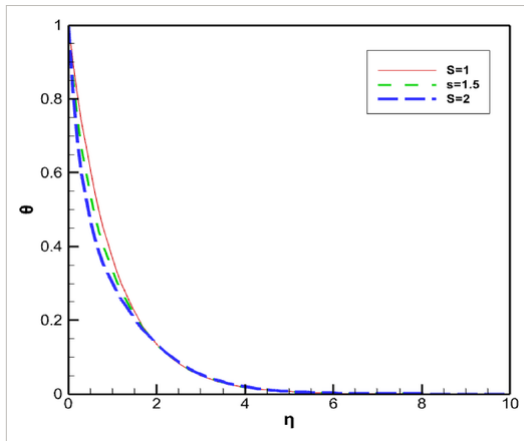


**FIGURE 5**

[Open in figure viewer](#) | [PowerPoint](#)

Temperature profile for several values of  $S$  with  $\sigma = 1$

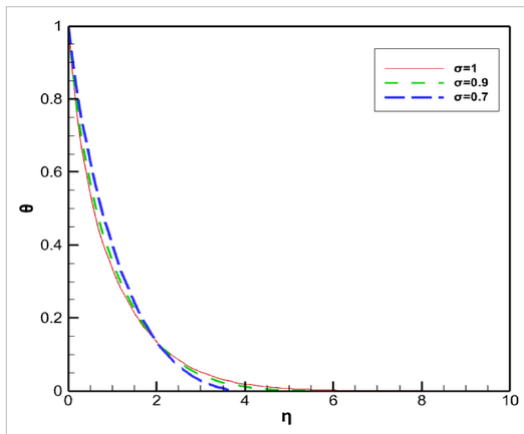


**FIGURE 6**

[Open in figure viewer](#) | [PowerPoint](#)

Temperature profile for several values of  $\sigma$  for  $K = 0.01$

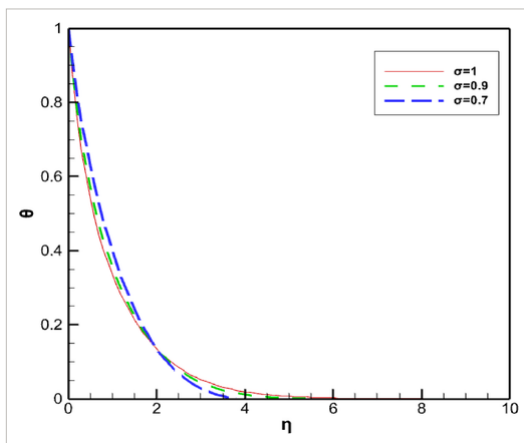


**FIGURE 7**

[Open in figure viewer](#) | [PowerPoint](#)

Temperature profile for several values of  $\sigma$  for  $K = 0.05$

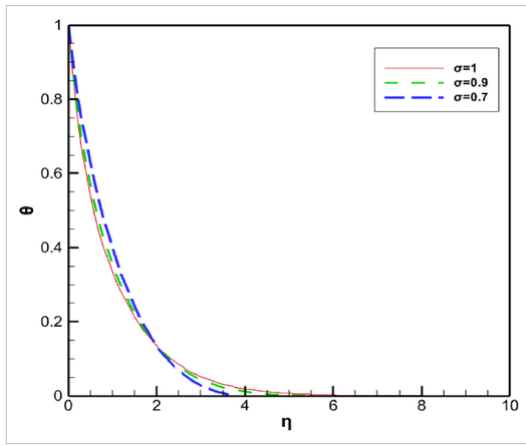


**FIGURE 8**

[Open in figure viewer](#) | [PowerPoint](#)

Temperature profile for several values of  $\sigma$  for  $K = 0.09$

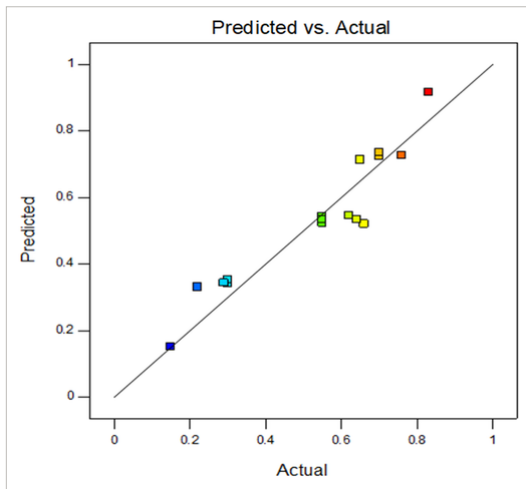


**FIGURE 9**

[Open in figure viewer](#) | [PowerPoint](#)

Contrast between predicted upshots and actual upshots for velocity

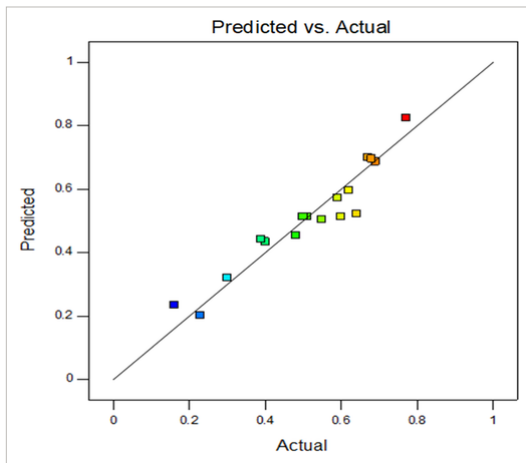


**FIGURE 10**

[Open in figure viewer](#) | [PowerPoint](#)

Contrast between predicted upshots and actual upshots for temperature

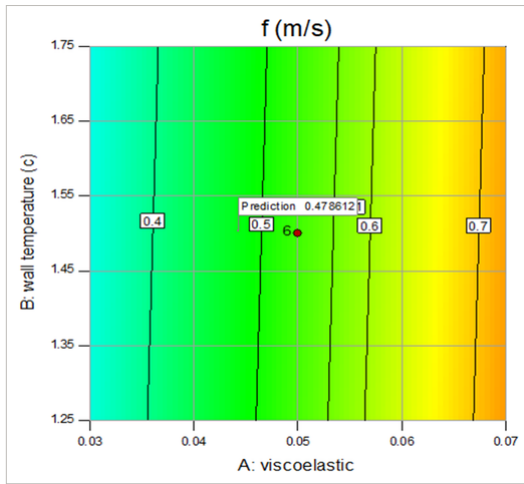


**FIGURE 11**

[Open in figure viewer](#) | [Download PowerPoint](#)

Two-dimensional graph response surface method in the velocity parameter for range of maximum wall temperature

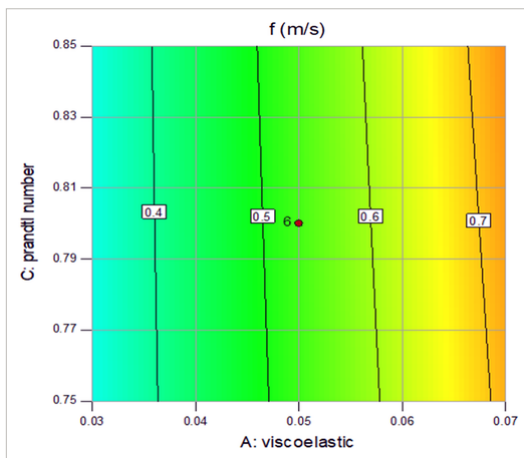


**FIGURE 12**

[Open in figure viewer](#) | [Download PowerPoint](#)

Two-dimensional graph response surface method in the velocity parameter for range of maximum Prandtl number

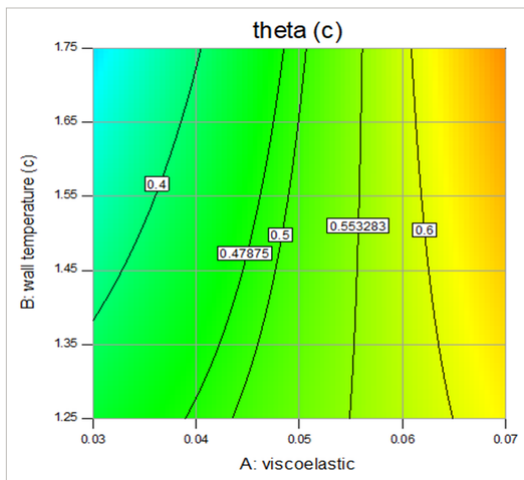


**FIGURE 13**

[Open in figure viewer](#) | [Download PowerPoint](#)

Two-dimensional graph response surface method in the temperature parameter for range of maximum wall temperature

According to Figures 11, 12, and 14 and in the state of the maximum velocity value, the modes of optimization evaluated between 10 experimental data as follows:

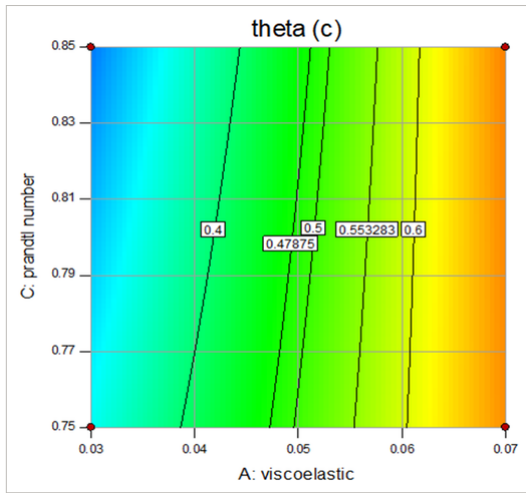


**FIGURE 14** [Open in figure viewer](#) | [PowerPoint](#)  
 Three-dimensional graph response surface method in the velocity parameter for range of maximum wall temperature

$K = 0.070, s = 1.750, \sigma = 0.850, f = 0.726, \theta = 0.696.$

By increasing the amount of  $K$ , the fluid velocity and fluid temperature 12% increased the ratio of the minimum viscoelastic parameter and reached the best optimizations value in the  $f = 0.7$  and  $\theta = 0.6$ . According to Figure 15, in the modes of maximum Prandtl number ( $\sigma = 0.850$ ) the best optimal mode occurred as follows:

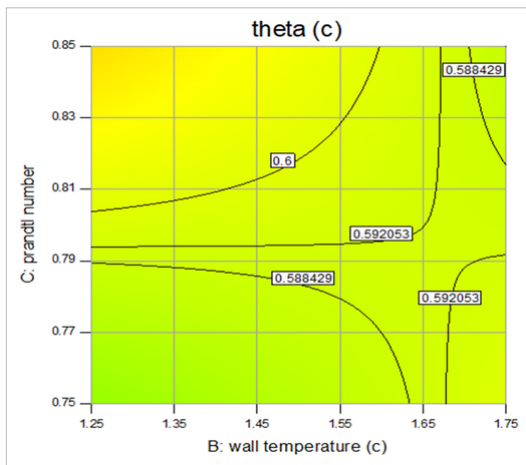


**FIGURE 15** [Open in figure viewer](#) | [PowerPoint](#)  
 Two-dimensional graph response surface method in the temperature parameter for range of maximum Prandtl number

$K = 0.070, s = 1.250, \sigma = 0.850, f = 0.736, \theta = 0.70.$

In this graph, the best optimization mode occurred in the  $K = 0.070, \sigma = 0.850$  with  $\theta = 0.70$ . By increasing the Prandtl number, the convection warm exchange 43% increased ratios of the minimum Prandtl number. According to Figure 16, in the modes of maximum wall temperature ( $s = 1.750$ ) the best optimal mode for fluid temperature and velocity occurred at  $f = 0.33$  and  $\theta = 0.23$ . In general and by balanced modes for Prandtl number and viscoelastic parameter and wall temperature, the best optimization occurred for fluid velocity and fluid temperature with  $f = 0.67$  and  $\theta = 0.606$ .

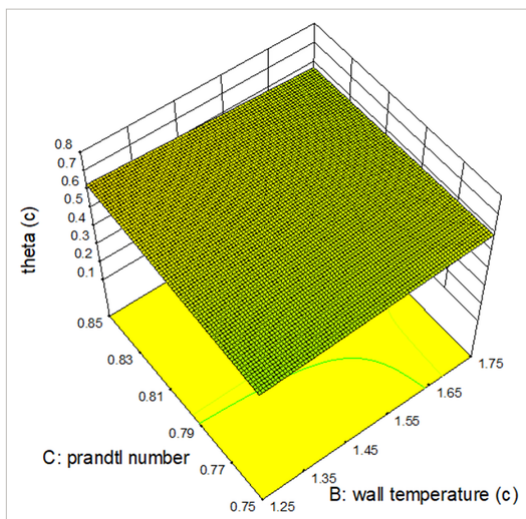


**FIGURE 16** [Open in figure viewer](#) | [PowerPoint](#)

According to Figures 16 and 17, by increasing the Prandtl number, the wall temperature decreased between  $x = 1.45$  and  $x = 1.75$ . In general, with passing the fluid flow from left to the right of the sheet, the amount of temperature decreased from  $T = 0.6$  to  $T = 0.59$ .

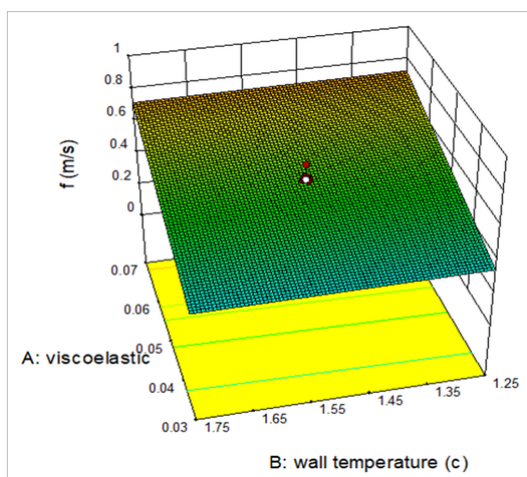


FIGURE 17

[Open in figure viewer](#) | [PowerPoint](#)

Three-dimensional graph response surface method in the temperature parameter for range of maximum wall temperature

## 7 CONCLUSION

This paper aimed at investigating the variation of heat transfer and velocity changes of the fluid flow along the vertical line on a surface drawn from both sides. In the beginning, several parameters such as Prandtl number and viscoelastic effect were evaluated for heat transfer and fluid velocity by the VIM method. The results were compared with the numerical method. The second part of the description relates to the use of RSM in the Design-Expert software.

By increasing the amount of  $K$ , the fluid velocity and fluid temperature 12% increased the ratio of the minimum viscoelastic parameter and reached the best optimizations value in the  $f = 0.7$  and  $\theta = 0.6$ .

By expanding the Prandtl number, the convection heat transfer 43% increased the ratio of the minimum Prandtl number.

The purpose of optimization research in this paper is to increase warm transfer and reduce fluid flow velocity in specific numbers

As the value of  $k$  increases, the value of fluid velocity indicates an increase and by increasing the Prandtl number, the value of temperature decreases.

## CONFLICT OF INTEREST

The authors declare no potential conflict of interest

## AUTHOR CONTRIBUTIONS

**Pooya Pasha:** Conceptualization (supporting); data curation (equal); formal analysis (equal); methodology (equal); project administration (equal); resources (equal); software (equal); supervision (equal); validation (equal); visualization (equal); writing – original draft (equal); writing – review and editing (equal). **Ali Hosin Alibak:** Supervision (equal); visualization (equal). **Hossein Nabi:** Validation (equal); writing – review and editing (equal). **Farzad Tat Shahdost:** Project administration (equal).

## Nomenclature

$\alpha$	Thermal diffusivity
$\mu$	Dynamic viscosity
$\rho$	Density of fluid
$\sigma$	Prandtl number
$\nu$	kinematic viscosity
$\theta$	Dimensionless temperature
$\eta$	Dimensionless variable
$w$	Condition at the surface
$\infty$	Condition at the free stream
$u, v$	Velocity components
$A(u)$	General differential operator
$L(u)$	Linear part of the Equation
$N(u)$	Nonlinear part of the equation
$g(r)$	known analytic function

NUM	Numerical method
HPM	Homotopy perturbation method
$p$	Embedding parameter
$T$	Temperature of fluid
$T_\infty$	Ambient fluid temperature
$T_w$	Stretching sheet temperature
$Ec$	Eckert number
$cp$	Specific heat
$k$	Viscoelastic parameter
$s$	wall temperature parameter
$x,y$	Space coordinates

Open Research ▼

#### PEER REVIEW

The peer review history for this article is available at <https://publons.com/publon/10.1002/eng2.12505>.

#### DATA AVAILABILITY STATEMENT

Data available on request from the authors

#### REFERENCES ▼

- Jha BK, Malgwi PB. Hall and ion-slip effects on MHD mixed convection flow in a vertical microchannel with asymmetric wall heating. *Eng Rep.* 2020; 2(9):e12241. [Wiley Online Library](#) | [CAS](#) | [Google Scholar](#)
- Oyem AO, Mutuku WN, Oke AS. Variability effects on magnetohydrodynamic for Blasius and Sakiadis flows in the presence of Dufour and Soret about a flat plate. *Eng Rep.* 2020; 2(10):e12249. [Wiley Online Library](#) | [Google Scholar](#)
- Oyelakin IS, Lalramneihmawii PC, Mondal S, Nandy SK, Sibanda P. Thermophysical analysis of three-dimensional magnetohydrodynamic flow of a tangent hyperbolic nanofluid. *Eng Rep.* 2020; 2(4):e12144. [Wiley Online Library](#) | [CAS](#) | [Google Scholar](#)
- Raju A, Ojjela O. Effects of the induced magnetic field, thermophoresis, and Brownian motion on mixed convective Jeffrey nanofluid flow through a porous channel. *Eng Rep.* 2019; 1(4):e12053. [Wiley Online Library](#) | [CAS](#) | [Google Scholar](#)
- Ibrahim W, Negera M. Melting and viscous dissipation effect on upper-convected Maxwell and Williamson nanofluid. *Eng Rep.* 2020; 2(5):e12159. [Wiley Online Library](#) | [CAS](#) | [Google Scholar](#)
- Kishan N, Dessie H. MHD effects on heat transfer over stretching sheet embedded in porous medium with variable viscosity. *Ain Shams Eng J.* 2014; 5: 3967- 3977. [Google Scholar](#)
- Shateyi S. Numerical analysis of three-dimensional MHD Nanofluid flow over a stretching sheet with convective boundary conditions through a porous medium. In: MS Kandelousi, ed. *Nanofluid Heat and Mass Transfer in Engineering Problems*. InTech; 2016. [Google Scholar](#)
- Makinde OD, Khan ZH, Ahmad R, Khan WA. Numerical study of unsteady hydro magnetic radiating fluid flow past a slippery stretching sheet embedded in a porous medium. *Phys Fluid.* 2018; 30: 30345- 30354. [Crossref](#) | [Google Scholar](#)
- Jalilpour B, Jafarmadar S, Ganji DD, Shotorhan AB, Taghavifar H. Heat generation/absorption on MHD stagnation point of nanofluid towards a porous stretching sheet with prescribed surface heat flux. *J Mol Liquid.* 2014; 195: 194- 204. [Crossref](#) | [CAS](#) | [Google Scholar](#)
- Nadeem S, Hussain ST, Lee C. Flow of a Williamson fluid over a stretching sheet. *Braz J Chem Eng.* 2013; 30(03): 619- 625. [Crossref](#) | [CAS](#) | [Google Scholar](#)
- Cortell R. A note on flow and heat transfer of a viscoelastic fluid over a stretching sheet. *Int J Non-Linear Mech.* 2006; 41: 78- 85. [Crossref](#) | [Web of Science®](#) | [Google Scholar](#)
- Tousiflqra MI. Magnet of hydrodynamic free stream and heat transfer of nanofluid flow over an exponentially radiating stretching sheet with variable fluid properties. *Front Phys.* 2019; 15: 1- 11. [Google Scholar](#)
- Krishna MV, Ahamad NA, Chamkha AJ. Hall and ion slip effects on unsteady MHD free convective rotating flow through a saturated porous medium over an exponential accelerated plate. *Alex Eng J.* 2020; 59(2): 565- 577. [Crossref](#) | [Google Scholar](#)
- Khan M, Shahzad A. On boundary layer flow of a sisko fluid over a stretching sheet. *Quaest Math.* 2013; 36: 137- 151.

- 
- 15 Iqbal Z, Qasim M, Wais MA, Hayat T. Stagnation-point flow by an exponentially stretching sheet in the presence of viscous dissipation and thermal radiation. *J Aerospace Eng.* 2015; **29**: 1- 6.  
[Google Scholar](#)
- 
- 16 Fayyadh MM, Kandasamy R, Mohammed R, Abbood JA. The performance of Al<sub>2</sub>O<sub>3</sub> crude oil on nonlinear stretching sheet. *J Mech Cont Math Sci.* 2018; **13**: 1- 9.  
[Google Scholar](#)
- 
- 17 Dutta BK, Gutta AS. Cooling of a stretching sheet in a viscous flow. *Ind Eng Chem Res.* 1998; **26**(2): 333- 336.  
[Crossref](#) | [Google Scholar](#)
- 
- 18 Roslinamohd N, Amin N, Filip D, Pop L. Stagnation point flow of a micropolar fluid towards a stretching sheet conform. *Int J Non-Line.* 2004; **39**: 1227- 1235.  
[Crossref](#) | [Google Scholar](#)
- 
- 19 Ganji DD, Hatami M. Squeezing cu-water nanofluid flow analysis between parallel plates by DTM-pade method. *J Mol Liquid.* 2014; **193**: 38- 44.  
[Google Scholar](#)
- 
- 20 Khan WA, Pop I. Boundary – layer flow of a nanofluid past a stretching sheet. *Int J Heat Mass Transf.* 2010; **53**: 532477- 532483.  
[Crossref](#) | [Google Scholar](#)
- 
- 21 Tanzila H, Nadeem S. Induced magnetic field stagnation point flow of nanofluid past convectively heated stretching sheet with bouncy effects. 2016; **25**(11):114701.  
[Google Scholar](#)
- 
- 22 Bujurke NM, Biradar SN, Hiremath PS. Second order fluid flow past a stretching sheet with heat transfer. *Zangew Math Phys.* 1987; **38**: 38890- 38892.  
[Google Scholar](#)
- 
- 23 Ahmed M. *Steady Flow and Heat Transfer Due to Bidirectional Stretching Sheet.* LAP Lambert Academic Publishing; 2013 28.  
[Google Scholar](#)
- 
- 24 Pasha P, Nabi H, Ganji D. Davood, 1399, Analytical solution of non -Newtonian second –grade fluid flow by VIM and ADM methods on a stretching sheet. <https://civilica.com/doc/1170934> .  
[Google Scholar](#)
- 
- 25 Kachapi SHH, Ganji DD. Analysis of nonlinear equations in fluids, progress in nonlinear. *Science.* 2011; **2**: 1- 12.  
[Google Scholar](#)
- 
- 26 Ghadikolaei SS, Hosseinzadeh K, Yassari M, Sadeghi H, Ganji DD. Analytical and numerical solution of non-Newtonian second-grade fluid flow on a stretching sheet. *Thermal Sci Eng Progr.* 2018; **5**: 309- 316.  
[Crossref](#) | [Google Scholar](#)
- 
- 27 Chamoli S. Preference selection index approach for optimization of V down perforated baffled roughened rectangular channel. *Energy.* 2015; **93**: 1418- 1425.  
[Crossref](#) | [Google Scholar](#)

[Download PDF](#)

[About Wiley Online Library](#)

[Privacy Policy](#)

[Terms of Use](#)

[Cookies](#)

[Accessibility](#)

[Publishing Policies](#)

[Help & Support](#)

[Contact Us](#)

[Training and Support](#)

[DMCA & Reporting Piracy](#)

[Opportunities](#)

[Subscription Agents](#)

[Advertisers & Corporate Partners](#)

[Connect with Wiley](#)

[The Wiley Network](#)

[Wiley Press Room](#)